A Compact Hydrogen Maser with Exceptional Long-Term Stability

DAVID A. HOWE AND FRED L. WALLS

Abstract—A compact passive hydrogen maser with many unique features, including a significant reduction in size over previous hydrogen masers, is described. It uses the passive mode of operation, thereby permitting use of a small microwave TE_{011} cavity which is dielectrically loaded by a low-loss alumina (Al_2O_3). The cavity is 14.6 cm outside diameter and 13.7 cm high, and weighs only 4.4 kg. The unloaded-cavity Q factor is about 6000. With a conventional source, hexapole state selector, and four magnetic shields, the volume of the entire hydrogen maser resonator package is only about 20 l.

The FEP-coated quartz bulb which is common in other masers has been replaced by a similar coating on the inside wall of the cavity. This has yielded a simpler design and more rugged hydrogen maser package. The technique for the application of liquid emulsion FEP is discussed.

The cavity and attached endcaps compose the vacuum envelope, thus allowing use of a single vacuum system. The dimensional stability of the ceramic cavity under barometric changes is sufficiently within the range of the electronic cavity servo that a second vacuum system is not needed. For temperature control, a single oven is located in the magnetic shield nest.

The most recent stability data compiled from four compact hydrogen masers built at NBS is presented. Comparisons are made against the cesium standard NBS-4 and a time scale comprised of nine commercial cesium standards (denoted as 8s). The drift of the longest running measured maser (H4) is undiscernible when compared against the time scale (UTC) composed of NBS-4 with the 8s time scale for two 69-day measurement durations.

INTRODUCTION

Fig. 1. Magnetic hyperfine transition of hydrogen atom (above). Hydrogen maser schematic (below).

HYDROGEN MASER DEVELOPMENT in recent years has been directed toward a reduction in size without substantial compromise in frequency stability. Traditionally, the hydrogen maser has been an oscillator at approximately 1.42 GHz in the so-called "active" mode. However, a non-self-oscillating (or passive) configuration has been shown to reduce the long-term (greater than 10 days) drift and random-walk instabilities associated with active masers. The requirement for a high-Q RF cavity surrounding the interrogated volume of H-atoms is relaxed. This makes possible new hydrogen maser designs, one of which is outlined in this paper.

At NBS, the concept of the passive rather than active maser was developed in order to obtain better long-term stability than that observed using active maser designs [1]–[3]. A quartz oscillator is locked to the hyperfine resonance using a design

similar to optical pumping and atomic–molecular beam devices. Two important requirements of conventional self-oscillating masers have been relaxed: 1) a relatively high cavity Q (needed for oscillation), and 2) excellent cavity frequency stability as a function of temperature, pressure, varactor voltage, and time. Item 2) is possible because in the passive mode of operation one has the ability to lock the frequency of the cavity to the H resonance. Passive electronics have been successfully deployed on a conventional full-size maser [1], [2]. The development of these new electronics makes possible a reevaluation of the design used in the maser (the so-called "physics package").

The maser works on the magnetic dipole transition of the ground state of free hydrogen atoms contained in a storage volume. Fig. 1 shows the $F = 0$ and $F = 1$ ground electronic states as a function of applied magnetic field. This hyperfine transition in hydrogen has a frequency of approximately 1 420 405 751 Hz. RF interrogation of the hydrogen atoms at this frequency takes place within a teflon-coated storage

Fig. 2.   In the passive mode, the hydrogen maser is not oscillating. The NBS maser electronics use two servo systems involving the cavity (f_1 = 12 kHz) and the narrow H-line (f_2 = 12 kHz).
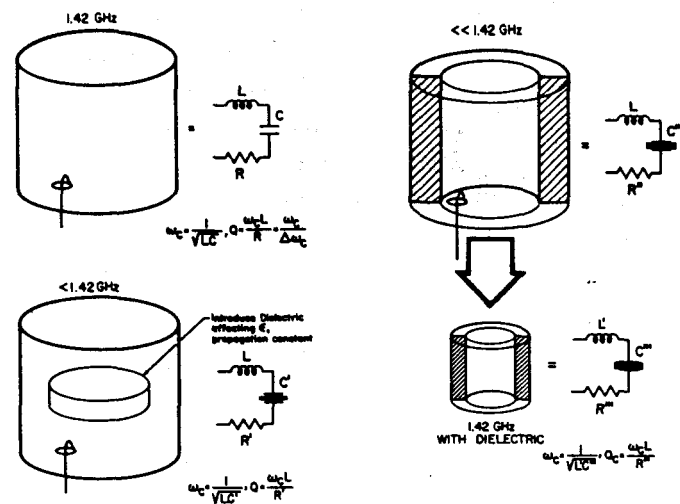

Fig. 3.   A small cavity is realized by the addition of low-loss alumina dielectric. The conventional hydrogen maser storage bulb is eliminated and the wall of the open center is coated with teflon.

volume. This wall-coating typically permits the hydrogen atoms to bounce 2×10^4 times within this volume before losing their phase relative to the RF magnetic field.

In order to achieve high-filling factors, the average value of the instantaneous RF magnetic field needs to be in a certain direction over the entire hydrogen storage volume. One can develop cavity designs which yield small size and relatively high filling factor over a given volume [3]–[6]. The cavity design used here is a right circular cylinder of low-loss ceramic with a bore down the central axis and a silver coating on the outside surface. The ends are capped with Al_2O_3 plates. The closed central bore is the hydrogen-storage volume. Along with a good filling factor, this geometry has the benefit of a high level of symmetry to better than 0.1 percent about all axes of the RF magnetic field in the storage volume. The TE_{011} mode is used. Therefore, in this new design, the microwave cavity forms the vacuum envelope and storage volume. With the loss given by currently available dielectric materials, this is only made possible because of the passive electronic scheme in which the maser is not oscillating.

Fig. 2 shows a block diagram of the passive maser scheme. A thorough explanation of the operation of the servo system is described in [1]–[3]. The interrogation (exciter) signal at 1420 MHz which enters the cavity is phase-modulated at two frequencies, f_1 and f_2. Frequency f_1 is a high-frequency (12-kHz) phase-modulation component used to probe the hydrogen cavity. Modulation component f_2 is used to probe the hydrogen resonance at 12-Hz modulation frequency. The two synchronously detected correction signals have different feedback time constants such that in the short term, the probe oscillator frequency is locked to the narrow hydrogen resonance. In the longer term, the cavity is tuned so that it is centered symmetrically about the probe frequency.

Full-size hydrogen masers typically also use a conventional

TE_{011} mode microwave cavity with a diameter of about 21 cm and length of about 50 cm. The lumped constant equivalent circuit for such a cavity consists of an inductance L in series with a capacitance C in series with a resistance R, as shown in Fig. 3. The insertion of a low-loss dielectric such as alumina (ceramic) affects the propagation constant, thus increasing C and decreasing the frequency of the cavity. The overall dimension of the cavity can then be reduced to compensate for the effect of the dielectric. RF symmetry, dielectric constant, overall dimension, and the hydrogen filling factor are all considered in order to achieve an optimum geometry. The net effect on the frequency of the TE_{011} mode must always be taken into account. Recall that the dielectric loading of the cavity affects the electric field. The RF magnetic H field (which excites the atoms) is uniquely determined relative to the orientation of the electric fields within the cavity by Maxwell's equations. It is possible to choose a cavity inside diameter so that the spatial average of the axial component of the oscillating H field does not reverse phase within this open storage volume. Consequently, the inside bore can substitute for the storage bulb used in a conventional maser with little compromise in the filling factor (see Fig. 4). The filling factor is 0.5.[1] A picture of the completed small maser cavity and shield assembly is shown in Fig. 4.

CAVITY COATING TECHNIQUE

The conventional hydrogen maser uses a quartz storage bulb with a teflon coating. The characteristics of hydrogen wall relaxation depend on the technique of coating application and the type and purity of teflon [7]. In the small passive maser, no quartz bulb is used and the coating is applied directly to the

---

[1] In the hydrogen maser, the filling factor is defined as

$$\eta = \frac{\langle B_z \rangle^2 \text{ storage}}{\langle B \rangle^2 \text{ cavity}}$$

where $\langle B_z \rangle^2$ storage is the mean value of the axial component of the amplitude of the magnetic field, averaged over the storage volume.

H-field is pinned by the
the perturbed E-field

A geometry is chosen so that
the oscillating H-field
does not reverse sign in the
open bore.

No bulb is needed to confine
the interrogated atoms to a
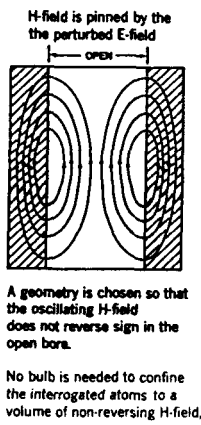volume of non-reversing H-field.

Fig. 4.   Completed prototype cavity assembly with four nested magnetic
shields.

inside wall of the ceramic dielectric. This is possible because
the phase of the axial component of the RF magnetic field does
not reverse in the hydrogen storage volume, but rather reverses
inside the dielectric. The coating serves two purposes. The first
is to provide a surface which minimally perturbs the phase of
the hydrogen atoms; the second is to vacuum seal and bond the
endcaps to the main cylinder.

The coating is made using Dupont FEP 120 emulsion.[2]
These resins in solution normally contain 50 percent water and
about 8 percent triton X-100 stabilizer. The stabilizer tends
to 1) keep the solid resin uniformly dispersed, and 2) lower the
surface tension by acting as a wetting agent. A new liquid
emulsion is then prepared by mixing 38 percent of the above
solution to 52 percent H_2O to 10 percent triton X-100 by vol-
ume. This new solution yields a thinner coat, slower initial
drying phase, and better wetting of the ceramic surface than
the original solution.

The liquid coating is applied to the ceramic endcaps with
a polypropelene squeeze bottle. The surface is uniformly wetted
and allowed to dry under a heat lamp for about 15 min. The
endcap is placed in a kiln with a heat rise of about +6 K/min.
Pure oxygen is flowed through the kiln during the heating
cycles. FEP 120 is fused by melting at a temperature of 360°C.
The rate of heating as one approaches 360°C is important
bcause the high thermal mass of the ceramic causes the ce-
ramic to lag the temperature of the kiln. Thus fusing of the
coating tends to first take place at the outside surface of the
coating, trapping stabilizers and other impurities within it. In
order to avoid this, the rate of temperature increase should be
reduced to approximately 1 K/min near 360°C.

Three layers of teflon are applied to the ceramic. This lowers
the probability that microscopic cracks will increase the ef-
fective surface area and that ceramic may be exposed at the
bottom of such cracks. Subsequent coats are applied by using
the previous mix and allowing the solution to dry to a very thin
overlayer. On the first wetting of the second and third coat,

milky lumps may tend to form but this is of no consequence.
After an initial dry, the solution is reapplied, wetting is more
pronounced, and the lumps dissolve. The surface then dries as
before in a uniform thin film, and the same kiln temperature
cycle is used. After the first coat the surface has a matte finish.
By the third coat the surface is glazed and clear.

The application of the teflon mix on the cylinder wall is the
same as the application on the endcaps. It is useful to mount
the cylinder in a lathe so that it can be rotated slowly while the
liquid solution rolls on the inside wall. The wall is first uni-
formly wetted, then removed from the lathe and allowed to
stand so that the liquid can drip to one end and the solution
allowed to dry. Glass endcaps fitted with tubes which go out
of the kiln are placed on the top and bottom of the cylinder
during the oven cycle so that oxygen can be flowed through the
inside bore of the cylinder. Here the oxygen serves two pur-
poses: 1) to oxidize the stabilizer, and 2) to keep the outside
surface of the coating cool relative to the temperature of the
heating ceramic cylinder. This is done to insure that fusing first
begins at the coating–ceramic boundary. A thermocouple is
mounted in one of the RF slots on the cavity sidewall to mon-
itor the temperature profile. Three layers are applied to the
inside wall of the cylinder. Layers can be removed by in-
creasing the oven temperature to about 650°C.

The same teflon used in the coating is also used as a glue to
bond the ceramic cylinder. The bonding process involves
wetting each endcap with its third (last) coat and fusing the
coat while the endcap is attached to the cylinder. A 3-kg weight
is placed on the endcap with the cylinder and endcap in an
upright position. This presses cylinder and endcap together as
the oven heats through the melting point and fusing temper-
ature of the coating. The resultant teflon-loaded gap between
endcap and cylinder is less than 25 μm (1 mil) thick, and the
vacuum seal allows pressures of below 10^{-9} torr in the cyl-
inder.

The hydrogen resonance linewidth is 1 Hz, thus yielding Q
$= 1.4 \times 10^9$. The storage volume is approximately 1 l. The
value of the fractional frequency wall shift has not been mea-
sured and is not considered consequential to the objectives of
high reproducibility of frequency and low drift. The fractional
wall frequency shift is estimated to be of the order of 1×10^{-11}
based on the work of others [7].

FREQUENCY STABILITY DATA

In all, four hydrogen masers (H1 through H4) of the type
described have been built at NBS. Frequency stability mea-
surements of each were made against NBS-4 (a cesium pri-
mary standard) wherever possible and against each other in
the case of H3 and H4. Some measurements have been re-
ported [8] and are summarized here in addition to new long-
term data on H3 and H4. H1 and H2 were not available si-
multaneously with H3 and H4 nor with each other since they
were transported to other facilities soon after their construc-
tion. However, data were taken for 30-day periods between H1
and H2, each against NBS-4. Other standards used in com-
parisons were nine commercial cesium clocks in a single in-
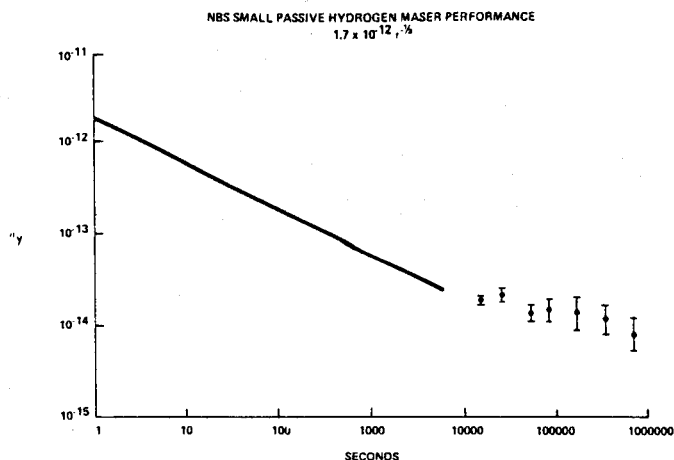dependent time scale denoted as 8s.

Fig. 5. Frequency stability of small hydrogen maser based on 32-day comparison simultaneously against 8s and a cesium standard NBS-4.

Fig. 6. Daily frequency of H3 versus NBS-4 (average frequency offset removed).

Identical designs were used for the four passive hydrogen masers. All had approximately the same hydrogen linewidths (between 1 and 2 Hz) and the same S/N ratios.

Short-term stability measurements (from 1 to 10 000 s) on the hydrogen masers consistently produced the straight solid line shown on the stability plot of Fig. 5. This is the white-frequency behavior of the masers at $1.7 \times 10^{-12} \tau^{-1/2}$ and is the stability referred to each individual hydrogen maser. NBS-4 had the same (individual) stability of about $1.7 \times 10^{-12} \tau^{-1/2}$.

Long-term data were compiled based on approximately 30-day uninterrupted comparisons between each maser, NBS-4, and 8s. These three sources were treated as independent clocks. By simultaneously comparing three independent clocks, it is possible to deduce the stability of each individual clock. The points shown in Fig. 5, which extend beyond averaging times of 10 000 s, represent the individual performance of H3 and H4 in a three-way intercomparison. The relation for determining the stability of an individual clock in a three-way comparison is [9]

$$\sigma_i^2 = \tfrac{1}{2}[\sigma_{ij}^2 + \sigma_{ik}^2 - \sigma_{jk}^2]. \tag{1}$$

The slight rise in σ_y at averaging times of about one-half day and one day are most likely attributable to environmental effects (diurnal variations). Day-to-day temperature and pressure changes appear to enter at about the 1×10^{-14} level. Although there is some degradation of stability for times around one day, the longer term stability is improving as shown by the last σ_y point at an averaging time of eight days (4 data samples). The eight-day value of σ_y is 8.1×10^{-15} ($\pm 5.6 \times 10^{-15}$).

Figs. 6 and 7 show the frequency fluctuations as a function of time for H3. Fig. 6 shows a comparison between H3 and NBS-4, and Fig. 7 is the comparison between H3 and 8s. A more graphic comparative measure is the residual time fluctuations indicated in Figs. 8 and 9. Over a 32-day data run, Fig. 8 shows the time residual (taken from day-to-day epoch data) between H3 versus NBS-4. The time residuals are the integrated fractional frequency fluctuations. Fig. 9 shows the same plot of time residuals between H3 and 8s. For these data, the
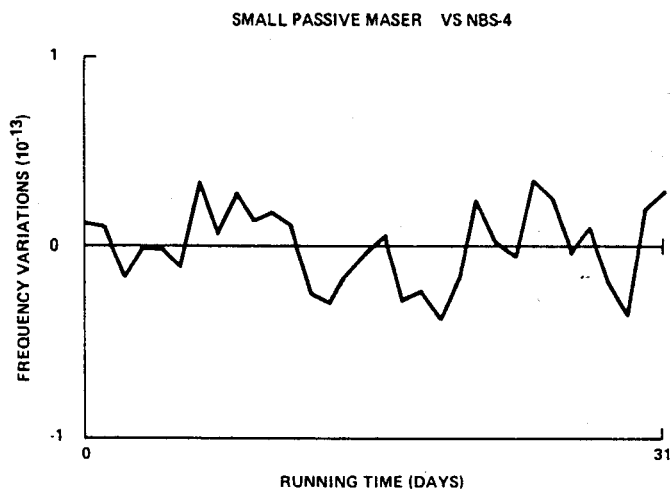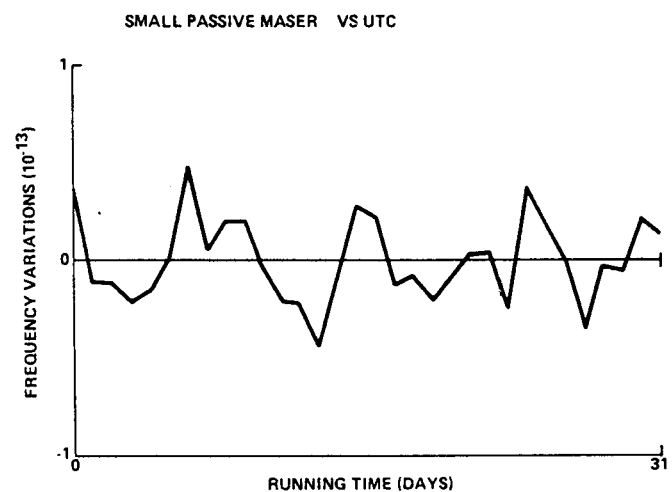

Fig. 7. Daily frequency of H3 versus 8s (average frequency offset removed).

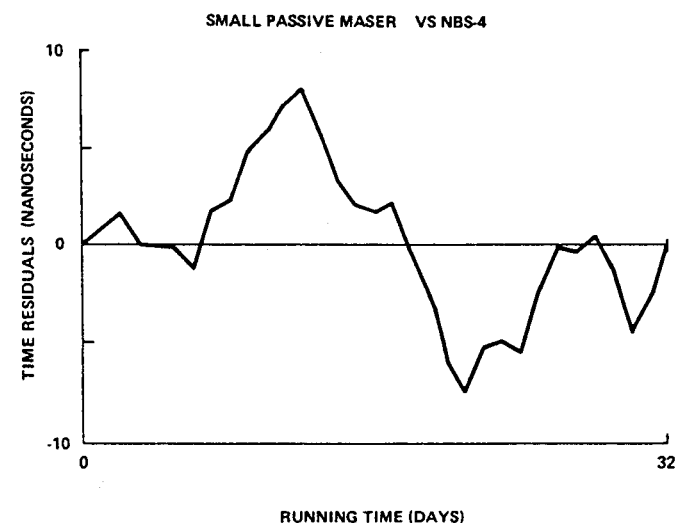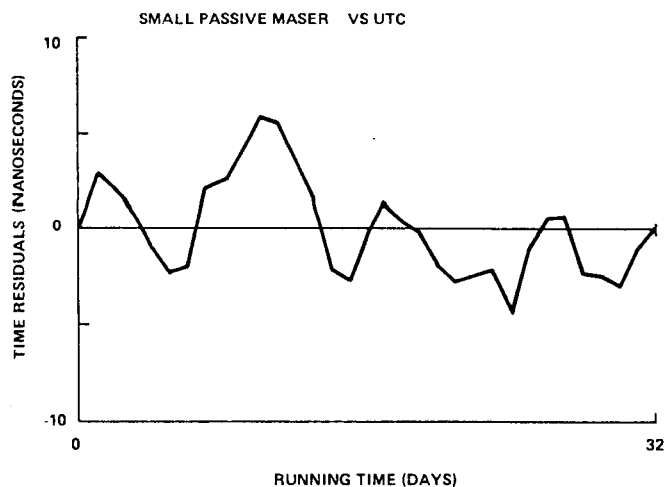Fig. 8. Daily time of H3 versus NBS-4 (average frequency offset removed).

SMALL PASSIVE MASER   VS UTC

Fig. 9.   Daily time of H3 versus 8s (average frequency offset removed).

TABLE I
SUMMARY OF SMALL PASSIVE MASER PERFORMANCE

EFFECT	OFFSET	INSTABILITY
1. Resonator Temperature Sensitivity	3×10^{-14}/K	2×10^{-15}/K
2. Spin Exchange	2×10^{-13}	2×10^{-15}
3. Magnetic Field	1×10^{-13}	10^{-15}
	for $\pm 3 \times 10^{-5}$ T	
	(± 0.3G)	
4. Power Dependence(microwave)	10^{-13}/dB	10^{-15}
5. Phase Modulator Drive	10^{-13}/dB	10^{-15}

Frequency Stability: ~$1.7 \times 10^{-12} \tau^{-\frac{1}{2}}$, 1s to 10^5s

Drift vs. UTC(NBS): ~1×10^{-15}/day (measurement limited)

fluctuations are noticeably smoother in the comparison to the UTC ensemble of nine cesium clocks. The end points for these runs of data are deliberately set to return to zero time difference, thus removing an average frequency offset. In this 32-day data set, there appears to be correlated frequency changes of parts in 10^{15} with period of the order of seven days. This possible effect is under further study.
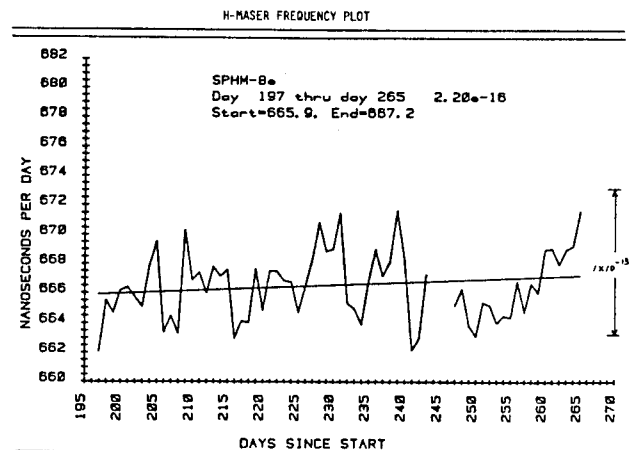
Environmental temperature and barometric pressure measurements were made coincident with frequency in order to determine the level of sensitivity to these environmental effects. Interestingly, there is no perceivable barometric pressure effect to the 1×10^{-14} level limited by the length of the data set. The barometric pressure changed by 7 percent (maximum) during this 32-day comparison. Other parameters were adjusted and their effects on the maser frequency are summarized in Table I.

DRIFT

The long-term measurements presented in Fig. 7 represent a 32-day accumulation of data soon after the construction of

H-MASER FREQUENCY PLOT

(a)

H-MASER FREQUENCY PLOT

(b)

Fig. 10.   (a) Daily frequency of H4 versus 8s (raw data) first 69 days. (b) Daily frequency of H4 versus 8s (raw data) second 69 days after magnetic shield degauss.

H3. In these data, a linear drift term of 4×10^{-15}/day was observed and removed from the data, so the plot is the residual fractional frequency fluctuations. After degaussing, however, another measurement of 17 days was made which exhibited a drift versus UTC(X) of 7×10^{-16}/day $\pm 2 \times 10^{-15}$/day for H3 (UTC(X) is 8s with NBS included).

Fig. 10 shows the daily frequency fluctuations between H4 and 8s. The total number of days reported is about 200 with an interruption for magnetic shield degaussing. This was done because of a large magnet which was moved in the vicinity of H4, and as one sees from Fig. 10, there was an accompanying frequency change after degaussing.

It should be noted that except for one interruption to degauss the magnetic shields, H4 operated continuously for eight months at NBS, Boulder. Also H4 has not been adjusted or touched during this period.

The data presented in Fig. 10 are raw data; no drift has been removed and the measurement bandwidth is over 100 Hz. A linear drift has been fitted to two segments of the data. The first 69 days yield drift of -1.82×10^{-16}/day. The second 69 days yield $+2.20 \times 10^{-16}$/day. These results are remarkable

for a hydrogen maser, and we conclude that the net drift is still below our ability to measure. In a comparison against UTC(NBS) the passive hydrogen maser₃ showed no discernible drift over several weeks. The uncertainty in this level is about 2×10^{-15}/day over several weeks limited by the day-to-day fluctuations of UTC(NBS). If one assumes the drift is half the uncertainty, one can reasonably assume the drift to be no worse than 1×10^{-15}/day.

Random walk best characterizes the very long-term fractional frequency instabilities. Environmental changes of temperature and pressure appear to affect the maser stability at the 1×10^{-14} level.

CONCLUSION

In this paper, frequency stability measurements on four passive hydrogen masers versus NBS-4 and UTC(NBS) have been presented. Frequency stability level is $1.7 \times 10^{-12} \tau^{-1/2}$ from 1 to 10^5 s. No drift above 1×10^{-15}/day has been detected; this value is limited by measurement uncertainty of 2×10^{-15}/day. Some environmental sensitivity (pressure and temperature) affects frequency stability at about the 1×10^{-14} level and the long-term (above 2×10^5 s) noise behavior is characterized as random walk. The long-term stability measurements presented here indicate great potential for the passive maser design as a clock and we are continuing to take measurements of H4 versus NBS-4 and UTC(NBS).

REFERENCES

[1] F. L. Walls and H. Hellwig, "A new kind of passively operating hydrogen frequency standard," in *Proc. 30th Ann. Symp. on Frequency Control*, p. 473, 1976.
[2] F. L. Walls, "Design and results from a prototype passive hydrogen maser frequency standard," in *Proc. 8th Ann. Precise Time and Time Interval (PTTI) Planning Meet.*, p. 369, 1976.
[3] D. A. Howe, F. L. Walls, H. E. Bell, and H. Hellwig, "A small, passively operated hydrogen maser," in *Proc. 33rd Ann. Symp. on Frequency Control*, p. 554, 1979.
[4] H. T. M. Wang, J. B. Lewis, and S. B. Crampton, "Compact cavity for hydrogen frequency standard," in *Proc. 33rd Ann. Symp. on Frequency Control*, p. 543, 1979.
[5] E. M. Mattison, E. L. Blomberg, G. U. Nystrom, and R. F. C. Vessot, "Design, construction, and testing of a small passive hydrogen maser," in *Proc. 33rd Ann. Symp. on Frequency Control*, p. 549, 1979.
[6] H. E. Peters, "Small, very small, and extremely small hydrogen masers," in *Proc. 32nd Ann. Symp. on Frequency Control*, p. 469, 1978.
[7] J. Vanier and R. Larouche, "Comparison of the wall shift of TFE and FEP teflon coating in the hydrogen maser," *Metrologia*, vol. 14, p. 31, 1978.
[8] F. L. Walls and D. A. Howe, "Precision timekeeping using a small passive hydrogen maser," in *Proc. 12th Annual Precise Time and Time Interval (PTTI) Planning Meet.*, 1980.
[9] J. A. Barnes, A. R. Chi, L. S. Cutler, D. J. Healey, D. B. Leeson, T. E. McGunigal, J. A. Mullen, Jr., W. L. Smith, R. L. Sydnor, R. F. C. Vessot, and G. M. R. Winkler, "Characterization of frequency stability," *IEEE Trans. Instrum. Meas.*, vol. IM-20, p. 105, 1971.